Chemical Engineering Journal 379 (2020) 122391

Contents lists available at ScienceDirect

Chemical Engineering Journal

journal homepage: www.elsevier.com/locate/cej

Facile one-step preparation of robust hydrophobic cotton fabrics by covalent bonding polyhedral oligomeric silsesquioxane for ultrafast oil/water separation

Yang Deng, Di Han*, Yi-Yi Deng, Qin Zhang, Feng Chen, Qiang Fu*

College of Polymer Science & Engineering, State Key Laboratory of Polymer Materials Engineering, Sichuan University, Chengdu 610065, PR China

HIGHLIGHTS

- A robust POSS based hydrophobic fabric was fabricated in a single-step.
- The POSS modified fabric exhibited excellent UV, chemical and mechanical stability.
- The POSS modified fabric can separate oil/water mixture with ultrafast oil permeation flux up to 114,744 $L{\cdot}m^{-2}{\cdot}h^{-1}$.

GRAPHICAL ABSTRACT

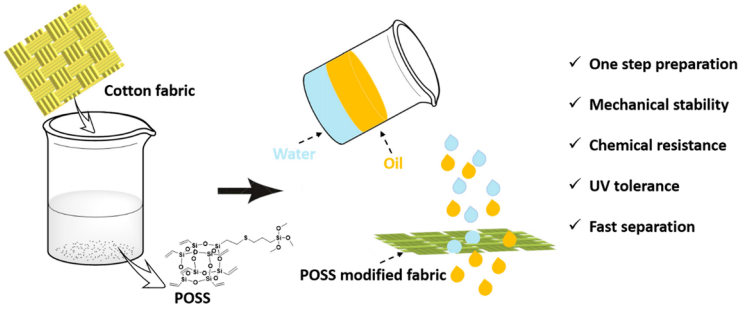

ARTICLE INFO

Keywords:
Polyhedral oligomeric silsesquioxane
Oil/water separation
Coating
Durability
High flux

ABSTRACT

Nowadays, oil contamination has become a major source of water pollution and results in the global environmental challenge. Although numerous efforts have been made on the fabrication of oil/water separation materials, their practical applications are still hindered by the low preparation efficiency, weak mechanical durability, poor chemical tolerance and environmental resistance, as well as low permeation flux. To overcome these drawbacks, herein, we directly anchor hydrophobic/oleophilic polyhedral oligomeric silsesquioxane (POSS) onto the surface of cotton fabric by one-step dipping strategy to yield a robust POSS based hydrophobic oil/water separation membrane. At First, commercially available octavinyl-POSS (VPOSS) was functionalized by 3-mercaptopropyltrimethoxysilane (MPTMS) via thiol-ene click reaction to afford a novel POSS derivate, named POSS-MPTMS. Then, it was used for modification of the cotton fabric by one-step dip-coating method to form a stable and robust POSS layer. The formed POSS layer endow modified cotton fabric become hydrophobic with the water contact angle higher than 142°. More importantly, the POSS modified fabric can withstand UV irradiation, chemical corrosion, ultrasonic washing as well as repeatedly mechanical abrasion for a long time. Solely driven by gravity, the modified fabric can enable separation of oil/water mixture with a permeation flux as high as 114,744 $L{\cdot}m^{-2}{\cdot}h^{-1}$. Moreover, it maintains excellent stability and effective separation property even in harsh environments with high concentration of acid, alkali, and salt solutions. We believe this facile strategy is a good solution for construction of advanced filtration materials for practical oil/water separation.

* Corresponding authors.
E-mail addresses: russell.d.han@outlook.com (D. Han), qiangfu@scu.edu.cn (Q. Fu).

https://doi.org/10.1016/j.cej.2019.122391
Received 15 June 2019; Received in revised form 28 July 2019; Accepted 30 July 2019
Available online 31 July 2019

1. Introduction

Oil contamination, as a major source of water pollution, becomes a global environmental challenge because of the increasing oily wastewater generated from our daily life, industrial production and oil spills [1–3]. For example, more than 720 thousand tons of crude oil was spilled in the Gulf of Mexico oil spill in 2010, which caused great economic loss to local sea creatures, fishery industry [4]. Besides, more than 140 KL oily wastewater can be discharged from a typical mining operation [5]. Thus, dealing with the oily wastewater in an effective and rapid way has become an urgent problem for water purification.

In recent years, a variety of techniques have been developed and membrane separation technology has been considered as promising approach for oil/water separation because of the intrinsic advantages of environmental friendly, energy saving and continuous operation [6–10]. In principle, the separation membrane shall possess hydrophobic/oleophilic surface as well as interconnected porosity that allows oil phase to permeate through easily while water phase cannot [11]. A good oil/water separation membrane shall meet the following requirements: (i) high separation efficiency and fast separation rate; (ii) excellent mechanical strength, chemical stability and environmental tolerance that can be used repeatedly in a long time under harsh environments; (iii) the preparation way should be convenient, scalable, environmental friendly and cost-effective [12]. To date, a variety of separation membranes have been fabricated [13–17], while the most popular approach is coating nanoparticles and low surface energy materials onto various substrates such as fabrics/textiles and metallic meshes [18–21]. Among them, cotton fabric has been considered as a good substrate for the preparation of oil/water separation membrane owing to its excellent mechanical property, good chemical resistance, intrinsic micro/nanoscale surface, large interconnected pore, good reactivity (massive hydroxyl groups), low cost and abundant production. However, the surface wettability of cotton fabric should be modified before use due to its inherent hydrophilic and oleophilic. To modify the surface wettability of cotton fabric, various nanoparticles including SiO_2 [22], TiO_2 [23,24], MnO_2 [25], Cu-Fe oxide [26], and polyaniline [27] combining fluorinated alkyl silane have been used for construction of hydrophobic surfaces and applied for oil/water separation. Nevertheless, their practical applications are hindered by some disadvantages. Specifically, these nanoparticles can be easily detached from substrates after mechanical rubbing owing to the weak interactions between them. Meanwhile, the fluorinated alkyl silanes are harmful for the environment and human beings. In addition, the fluorine-containing materials often cause the reduced permeation flux of membrane [20]. Thus, there is a constant demand for seeking out a facile and environmentally friendly method to fabricate robust and durable separation membrane with high permeation flux that can be used under harsh conditions.

Polyhedral oligomeric silsesquioxanes (POSS) are organic-inorganic hybrid nanoparticles with the molecular formula of $(RSiO_{1.5})_n$ [28–30]. The rigid inorganic siloxane core endows POSS with good mechanical properties [31–33], thermal stability [34–37], UV resistance [38,39] and low surface energy [40,41], while the soft organic substitutes afford POSS with good reactivity [42–45]. These advantages making POSS can be used to decrease the surface energy and increase the surface roughness simultaneously for the fabrication of hydrophobic surface [46–49]. Compared with using POSS-containing polymers to construct hydrophobic surface, it is better to directly anchor large amount of POSS onto the surface of substrate. To achieve this, Wang et al. dissolved fluorinated-decyl POSS (FD-POSS) into fluorinated alkyl silane (FAS) to construct superhydrophobic/superoleophobic cotton fabric through dip-coating method [50]. The hydrophobic/oleophobic FD-POSS will be trapped into the product of hydrolyzed FD-POSS and FAS to form a durable and robust self-cleaning surface. However, it cannot be used for oil/water separation due to the hydrophobic/oleophobic properties. Very recently, Hou et al. used mercapto silanes to convert the hydroxyl groups of cotton fabric into thiol groups, followed by a thiol-ene click reaction, methacryl-heptaisobutyl POSS was successfully immobilized to obtain a robust superhydrophobic cotton fabric in two-steps [51]. It was found that the obtained fabrics could adsorb oil from water, while their performance for continuous separation of oil/water mixtures were not clear. Based on these analyses, it remains large space to develop robust POSS based hydrophobic/oleophilic fabrics for fast and continuous oil/water separation. Meanwhile, the preparation process should be further simplified and the chemicals should be eco-friendly. To achieve this, the key point is design and synthesis of novel POSS derivate with hydrophobic/oleophilic property.

In this work, we report our efforts on the preparation of robust POSS based hydrophobic cotton fabric from one-step dipping method. To directly immobilize hydrophobic/oleophilic POSS onto cotton fabrics, at first, we synthesized a novel POSS derivate via thiol-ene click reaction between octavinyl-POSS (VPOSS) and 3-mercaptopropyltrimethoxysilane (MPTMS) (Scheme S1), named POSS-MPTMS, which contains the mixed functionalities of vinyl and trimethoxysilane. The selection of MPTMS to modify VPOSS as it is an eco-friendly monomer that contains a thiol and a trimethoxysilane group, allowing the fast formation of POSS-MPTMS. Meanwhile, the trimethoxysilane group of POSS-MPTMS not only can react with hydroxyl groups of cotton fabric to form a stable POSS layer but also can hydrolyze among themselves to form micro/nano surface roughness. In addition, the vinyl groups onto POSS cage can provide the substrates with good oleophilic. Then, POSS-MPTMS was applied to react with cotton fabric after an efficient dip-coating strategy (Scheme 1), and the reaction conditions such as monomer concentration and immersed time were explored. After that,

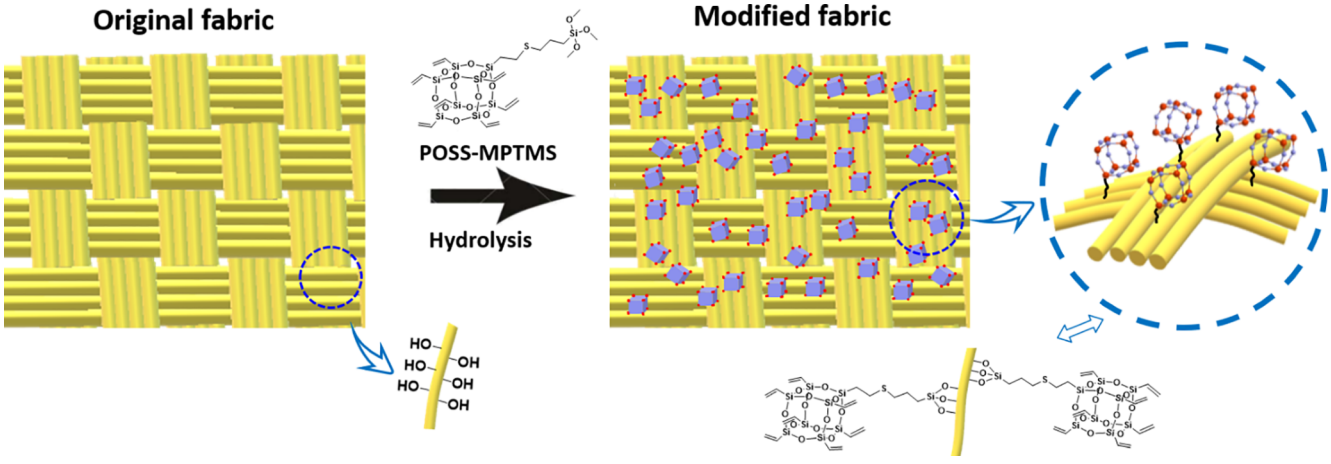

Scheme 1. Illustration of the fabrication process of POSS modified fabric.

the properties of modified fabrics were investigated, including the UV, solvents, abrasion resistance and acid-base tolerance. Finally, the modified fabric was applied for adsorption and separation of oil from water. We found that the modified fabric could separate different oil/water mixtures with high flux and separation efficiency only driven by gravity, even in harsh conditions (acid, alkali, and saturated salt solutions) for a long time.

2. Experimental section

2.1. Materials

The following chemicals were used as received: octavinyl-POSS (VPOSS, 98%) was purchased from Beijing HWRK Chemical Co., LTD, 3-mercaptopropyltrimethoxysilane (MPTMS, 97%) and 2,2-dimethoxy-2-phenylacetophenone (DMPA, 98%) were obtained from J&K Chemicals. Petroleum ether (PE), methanol (MeOH), dichloromethane (DCM), chloroform, tetrahydrofuran (THF), *N, N′*-dimethylformamide (DMF), acetone, N-hexane, Congo Red (CR), Sudan III, sodium hydroxide (NaOH), sodium chloride (NaCl) and sulfuric acid (H_2SO_4) were provided by Chengdu Kelong Chemical Co., Ltd. Cotton fabrics were purchased from a local store, and all of them were ultrasonically washed in NaOH solution (2 wt%) and distilled water to remove the possible impurities and wax before being used.

2.2. Synthesis of POSS-MPTMS via thiol-ene click reaction

The synthetic route of POSS-MPTMS is shown in Scheme S1. Specifically, VPOSS (3.0 g, 4.74 mmol), MPTMS (0.93 g, 4.74 mmol) and DMPA (25 mg, 0.15 mmol) were added into a beaker (50 mL) with a magnetic stirring bar and dissolved in 50 mL dried THF. After complete dissolution, the mixture was reacted under UV light (λ = 365 nm) for 15 min. After that, the mixture was concentrated and purified through flash column chromatography on a silica gel by using PE/DCM (v/v = 2/1) as eluent to afford the product as colorless viscous liquid. Yield: 32%. ^{1}H NMR (400 MHz, $CDCl_3$, ppm): δ = 6.20–5.84 (m, 21H), 3.57 (s, 9H), 2.63 (m, 2H), 2.55 (m, 2H), 1.70 (dt, 2H), 1.08 (m, 2H), 0.76 (dd, 2H). ^{13}C NMR ($CDCl_3$, 100 M, Hz, ppm): δ = 137.01, 136.97, 128.67, 128.62, 50.52, 34.68, 25.76, 22.81, 13.16, 8.61. ^{29}Si NMR (79 MHz, $CDCl_3$, ppm): −42.3, −68.5, −80.2, −80.3.

2.3. Fabrication of POSS-MPTMS modified fabric

The fabrication process of POSS-MPTMS modified fabric is depicted in Scheme 1 and the details are as follows. At first, POSS-MPTMS was dissolved in MeOH/H_2O (v/v = 95/5) solution and stirred for 1 h to generate a homogeneous hydrolysis solution. Then, the clean cotton fabrics (diameter = 4 cm) were immersed into POSS-MPTMS solution for hours, and dried at 110 °C. After that, fabrics were washed with methanol for three times to obtain the POSS-MPTMS modified fabric.

2.4. Instrumentation and characterizations

The UV lamp used in this work is LUYOR-3109 (3 W*9, λ = 365 nm, USA). All of the NMR spectra were recorded on a Bruker 400 MHz NMR at 20 °C. Fourier transform infrared (FT-IR) spectrum was carried out on a Nicolet 6700 instrument (Nicolet Instrument Company, USA) in an attenuated total reflectance (ATR) mode. The surface morphologies and elemental distribution of the original and modified fabrics were observed by field emission-scanning electron microscopy (JSM-7500F/X-MAX50, Japan) and energy dispersive X-ray spectrometry (EDS, Euro Vector EA3000, Italy) apparatus, respectively. X-ray photoelectron spectroscopy (XPS) data were recorded on an Escalab 250Xi spectrometer (Thermo Fisher Scientific Inc., UK), equipped with an aluminum X-ray source. Survey scans (0–1200 eV) were utilized to identify the surface elemental compositions of the original and modified fabrics. Thermogravimetric analysis (TGA) was carried out on a thermo-analyzer instrument (TA Instruments Inc., USA) with a heating rate of 10 °C/min. Static water contact angle (WAC) measurements were carried out by using a contact angle measuring device (DSA25, Krüss, Germany) at room temperature. 4 μL of deionized water was dropped onto the surface of fabric for each test and a computer program from the equipment supplier was used to measure WCA. All of the WCA values were obtained after 15 s of droplets deposition and repeated at least five times at different spots for each sample. Transmission electron microscope (TEM) experiment was recorded on a Tecnai T20 TEM with an accelerating voltage of 120 kV on a digital CCD camera, the sample was embedded into epoxy resin and microtome before observation. The tensile properties were tested using an Instron 5567 universal tensile testing machine at room temperature with tensile rate of 5 mm/min. The specific surface area and pore volume of the original and modified cotton fabric were calculated using the mercury intrusion porosimeter (MIP, Pore Master 33, USA). Data shown in Figures represent the mean ± standard deviation of quintuplicate experiments.

2.5. Durability and stability evaluation of the modified fabric

To evaluate the chemical stability of modified fabrics, they were immersed into a variety of different pH values aqueous solution (ranging from 1 to 13) and different organic solvents including DMF, THF, MeOH, acetone and N-hexane for different time intervals and then the treated fabrics were cleaned with deionized water and dried at 60 °C for WCA measurements. UV resistance of the modified fabrics were evaluated by radiation it under an UV light with a distance of 1 cm for 24 h. The washing durability of the modified fabrics were ultrasonically treated in aqueous solution containing detergent (0.15 wt%) for 1 h and their WCA values were measured. To investigate the mechanical stability of modified fabrics, they were rubbed with a sandpaper (1000 mesh) which loaded a weight (200 g) and dragged back and forth (20 cm as a cycle) in one direction with a speed of 4 cm s^{-1}.

2.6. Oil/water separation experiments

Various oil/water mixtures including chloroform, N-hexane, DCM and toluene were used to prepare the oil/water mixtures. The modified fabric was fixed on the bottom of a tube with an effective separation area of 7.03 cm^2. An oil/water mixture containing 20 mL of oil (dyed by Sudan III) [52] and 20 mL of water. The separation efficiency (η (%)) was evaluated by calculating the oil rejection coefficient according to eq. (1):

$$\eta\ (\%) = \left(1 - \frac{C_1}{C_0}\right) \times 100 \tag{1}$$

where C_0 and C_1 are the oil concentration of oil/water mixture before separation and the oil concentration of collected water after separation, respectively [53].

The permeate flux (J, L $m^{-2}h^{-1}$) was calculated according to Eq. (2):

$$J = \frac{V}{At} \tag{2}$$

where V is the permeate volume, A is the active area, t is the permeate time (h) [49].

To evaluate the oil absorption capacity, the modified fabric was immersed into various types of oil, after achieving saturation, the fabric was taken out rapidly (to avoid evaporation) and weighed quickly. The weight gain (%) of the modified fabric was used for demonstration the oil absorption capacity [54], which was calculated according to Eq. (3):

$$\text{Weight gain}(\%) = \frac{m_1 - m_0}{m_0} \times 100 \tag{3}$$

where m_0 and m_1 are the weight of the modified fabric before and after adsorption, respectively.

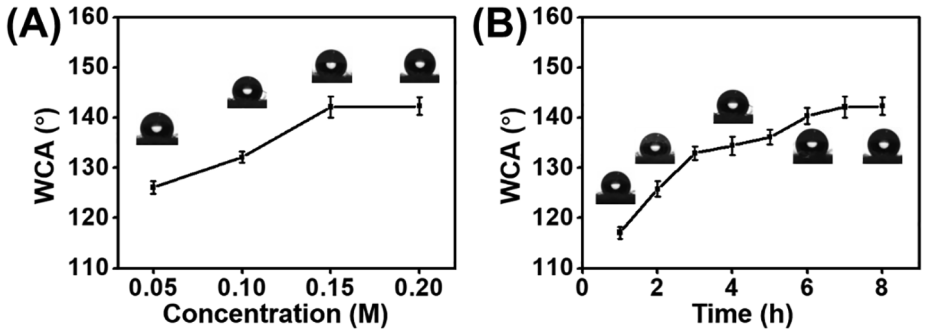

Fig. 1. The effect of different immersed (A) concentration (the immersed time is 7 h) and (B) time (the immersed concentration is 0.15 M) of POSS-MPTMS on water contact angle (WCA) of modified fabric. Error bars represent the standard deviation of quintuplicate experiments.

It should be noted that each test was repeated for five times and the modified fabric for cycle test was dried at 60 °C before using.

3. Results and discussion

3.1. Effect of the concentration of POSS-MPTMS and immersed time on the wettability of modified fabric

The method for construction of the POSS modified fabric is shown in Scheme 1. At first, a commercially available VPOSS was modified by MPTMS via thiol-ene reaction to yield the monoadduct product, namely POSS-MPTMS (Scheme S1). The chemical structure of POSS-MPTMS was identified by ^{1}H, ^{13}C, and ^{29}Si NMR spectra (Fig. S1). Then, a piece of cotton fabric was immerged into the POSS-MPTMS/MeOH/H_2O solution. During this process, dehydration occurred between the OH groups on the surface of cotton fabric and POSS-MPTMS, which result in the hydrophobic POSS nanoparticles were successful bonded onto the cotton fabric surface to afford the POSS modified fabric. We investigated the concentration of POSS-MPTMS and immersed time for the wettability of cotton fabric (Fig. 1). It was found that the WCA values of fabric were correlated with the concentrations of POSS-MPTMS and reaction times. The concentration of 0.15 M and 7 h of reaction time are the optimal conditions for modification of the cotton fabric (Fig. 1A and B), and the WCA of modified fabric can reach to around 142° after modification by POSS-MPTMS. The reason for cotton fabric becoming hydrophobic is due to the inherent low surface tension of POSS, which results in the lowered surface tension of modified fabric.

3.2. Surface chemical composition of the modified fabric

The wetting performance of a surface is closely related to its chemical composition. Therefore, the surface chemical composition of the original and modified fabrics was identified by FT-IR and XPS experiments. As displayed in Fig. 2A, the absorption band between

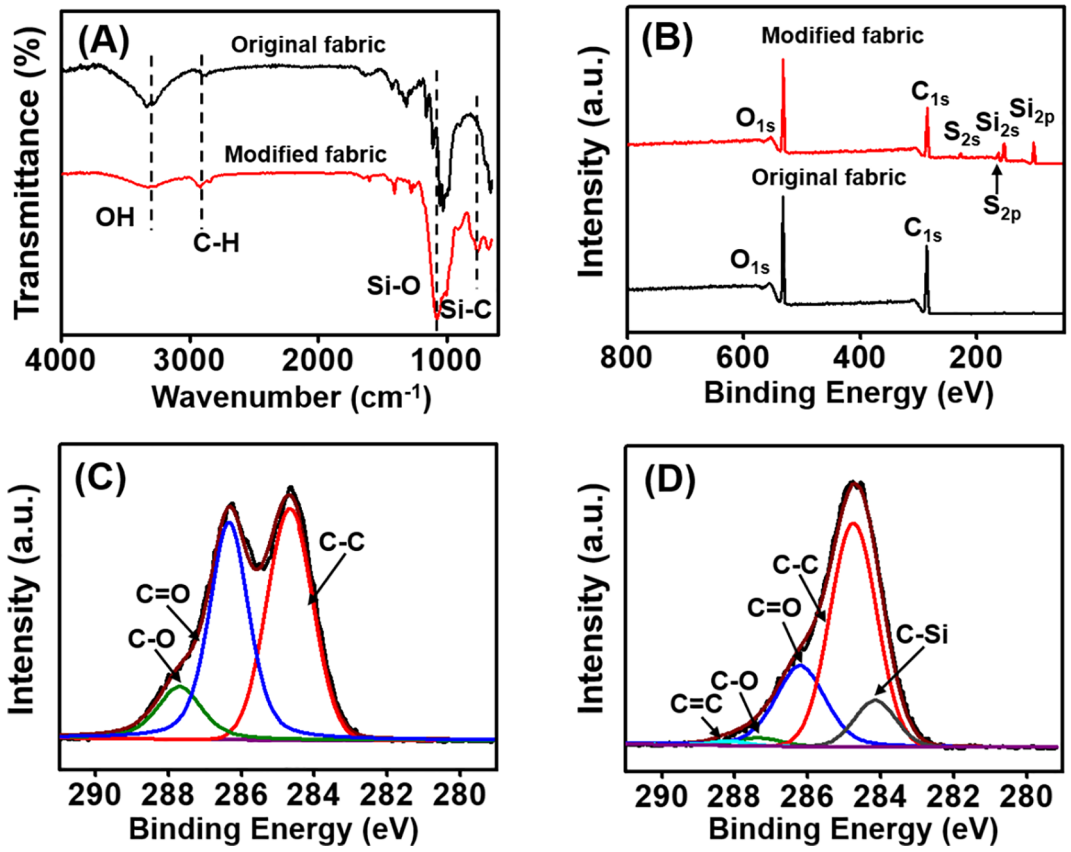

Fig. 2. (A) FT-IR and (B) XPS spectra of the original and modified fabrics. Highly resolution C_{1s} spectra of (C) the original fabric, (D) the modified fabric.

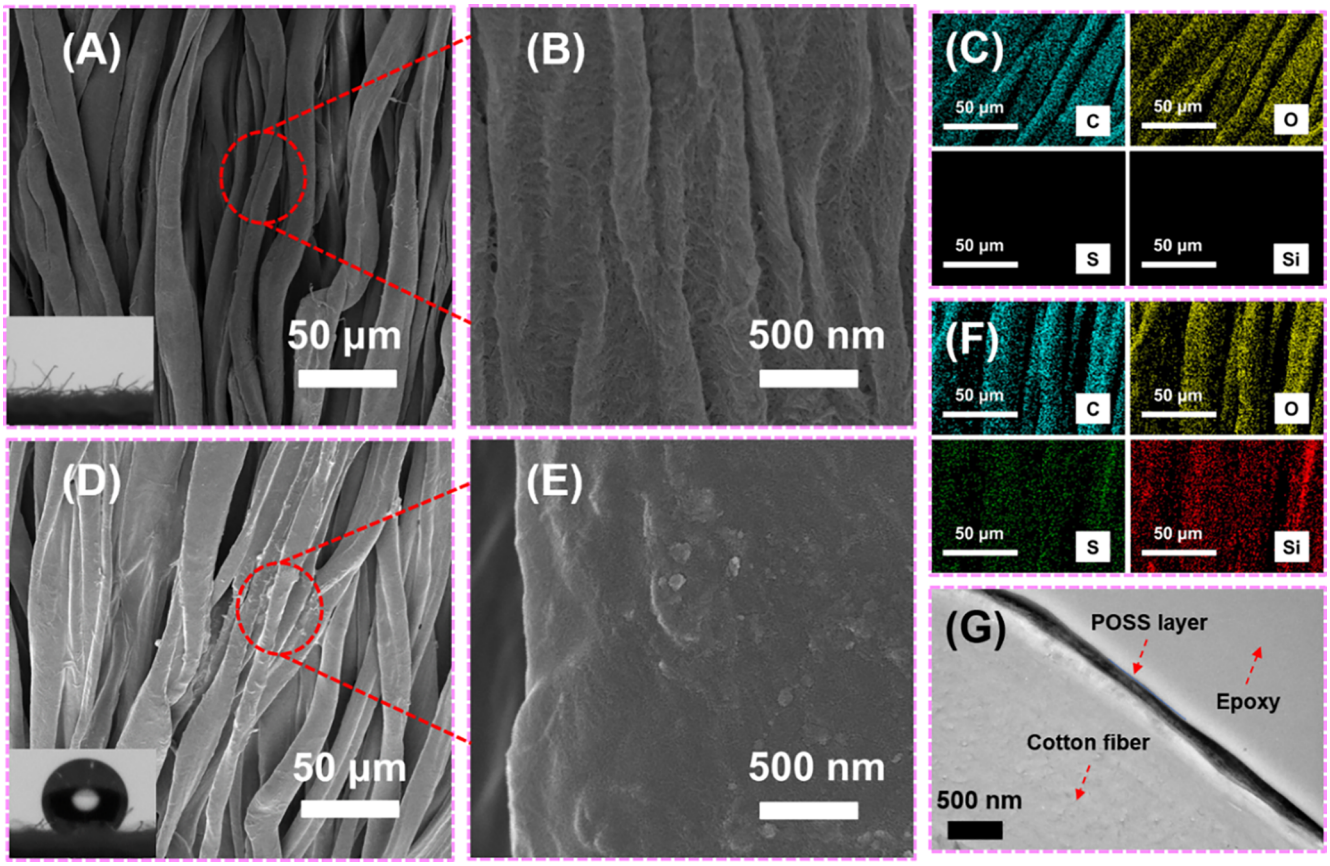

Fig. 3. Surface morphology of (A, B) the original and (D, E) the modified fabric surfaces, insets: images of their corresponding WCAs. EDS mapping images of (C) the original and (F) the modified fabric surfaces. (G) TEM image of the POSS layer coated on the modified fabric, which were prepared by microtome along the fiber axis direction.

3000 cm^{-1} and 3700 cm^{-1}, attributed to the stretching vibrations of hydroxyl groups, was weaken after the surface modification [55]. The absorption peak at 2905 cm^{-1}, 1617 cm^{-1} and 1408 cm^{-1} were contributed to the stretching vibrations of C–H, C = O, C-O of the cotton fabric substrate, respectively [56]. For the modified fabric, there are emerging two new peaks at around 1075 cm^{-1} and 780 cm^{-1}, the former is assigned to the stretching vibrations of Si-O linkage, and the latter is assigned to the Si-C bond [39]. It was found that only C and O elements were detected from the original fabric, while C, O, Si and S elements were observed from the modified fabric (Fig. 2B). As shown in Fig. 2C, the highly resolution C_{1s} peak of the original fabric displays three distinct peaks at about 284.8 eV, 286.4 eV and 287.8 eV, which are assigned to the C—C, C—O and C═O bonds, respectively [57]. In addition, the appearance of new peaks of C-Si bond (284.1 eV) and C═C bond (288.6 eV) for the modified fabric further indicated that POSS-MPTMS was successfully incorporated onto the cotton fabric (Fig. 2D). By calculating the elemental composition, we found that the amount of POSS-MPTMS coated on the fabric is ~3.0 wt%. Moreover, thermogravimetric analysis (TGA) suggested that the thermal stability and residual weight of the modified fabric were slightly higher than the original fabric (Fig. S2), with the POSS-MPTMS amount of ~2.9 wt% according to the data obtained from air condition. Based on these analyses, we conclude that POSS-MPTMS has been successfully grafted onto the surface of cotton fabrics.

3.3. Surface morphology of the modified fabric

The surface morphologies of the original fabric and modified fabric were observed by SEM. As shown in Fig. 3A and B, there are some intrinsic wrinkles on the surface of original fabric, the loaded water droplet can easily penetrate into the original fabric owing to the abundant hydroxyl groups on the cotton fabric that induces the hydrophilicity [58]. By contrast, the modified fabric surface become rough and relatively flat (Fig. 3D and E), and all of the C, O, Si and S elements are uniform distributed onto the surface of substrates (Fig. 3F). To acquire the thickness of coated POSS layer, the modified fabric was embedded into epoxy resin and microtomed for transmission electron microscope (TEM) observation. As shown in Fig. 3G and Fig. S3, there is no obvious roughness along the fiber axis and radial direction, and the thickness of coated POSS layer is around 100 nm. After loading a drop of water, it cannot permeate and remains spherical on the surface of the modified fabric with a WCA of 142°, which is attributed to the intrinsic micrometer morphologies of the fiber combine with hydrophobic POSS nanoparticles to form a hierarchical hydrophobic micro/nanostructure on the surface of the fabric.

3.4. Durability evaluation of the modified fabric

To meet the requirements of the practical application, the modified hydrophobic surfaces should be capable of maintaining adequate water-repelling ability after different physical and chemical destroys [59]. Therefore, the chemical stabilities of modified fabrics were investigated and illustrated in Fig. 4. The modified fabrics show high WCA values after treated in different pH values (from 1 to 13) for 72 h (Fig. 4A), suggesting the good water-repelling ability of modified fabrics. The WCA values show a slightly decline in high pH value region, which is due to the Si-O linkage are not stable in highly concentrated alkaline solution. Besides, the stability of fabrics in various organic solvents was also investigated. As shown in Fig. 4B, after soaked in various organic solvents for 72 h, WCA values of the surface has no significant change,

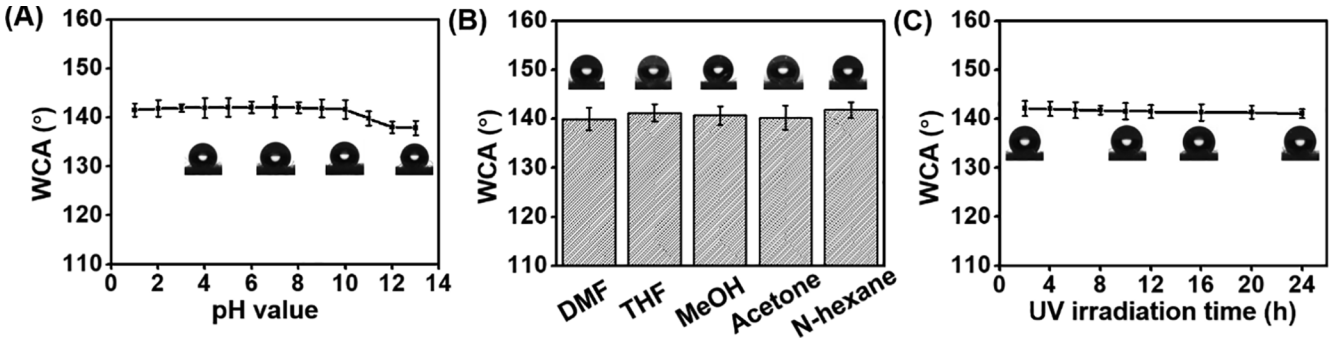

Fig. 4. The effect of (A) pH value, (B) solvents, and (C) UV irradiation time on the WACs of modified fabric. Error bars represent the standard deviation of quintuplicate experiments.

implying the modified surface is chemically stable. In addition, the modified fabrics exhibit excellent UV resistance. After radiated the modified fabric at UV light for 24 h, the measured WCA values can keep the same level compared to the initial state (Fig. 4C). The reason is attributed to the good UV resistance of POSS.

Besides, the durability of the hydrophobic surfaces should be taken into consideration in daily applications. Therefore, mechanical abrasion and washing resistance of the modified fabrics were evaluated. As shown in Fig. 5A, the modified fabric was put on a sandpaper (1000 mesh), subjected a load of 200 g, and the scratch experiment was performed by dragging the modified fabric back and forth (20 cm a cycle). As depicted in Fig. 5B, the WCA values of the modified fabric only show a slightly decline from 142.2° to 140.1° even after 180 cycles, still retaining its excellent anti-wetting property. Such outstanding mechanical durability of the modified fabric can be attributed to the rigid inorganic core of POSS and the formed silica networks. Besides, the modified fabric shows good washing resistance. When they are ultrasonically treated in detergent solution for long time, the measured WCA values are remaining unchanged (Fig. 5C), suggesting the fabric possesses excellent washing resistance. And the reason is attributed to the formed stable covalent bonds between cotton fabric and POSS-MPTMS.

The tensile properties of the modified fabric before and after treating at various conditions were also measured. As shown in Table 1, Figs. S4 and S5, compared to the original fabric, the tensile strength of modified fabric dropped from ~4396 N/cm^2 to ~3472 N/cm^2 (warp) and from ~1961 N/cm^2 to ~1550 N/cm^2 (weft), respectively. The decrease of tensile strength is mainly attributed to the formed POSS layer could reduce the water content of cotton fabric, resulting in the decreased amorphous region of cellulose matrix, ultimately weaken the tensile strength of modified fabric [60]. After treating the modified fabric under various conditions for a long time, their tensile strength have no obvious change. All of the treatments under harsh

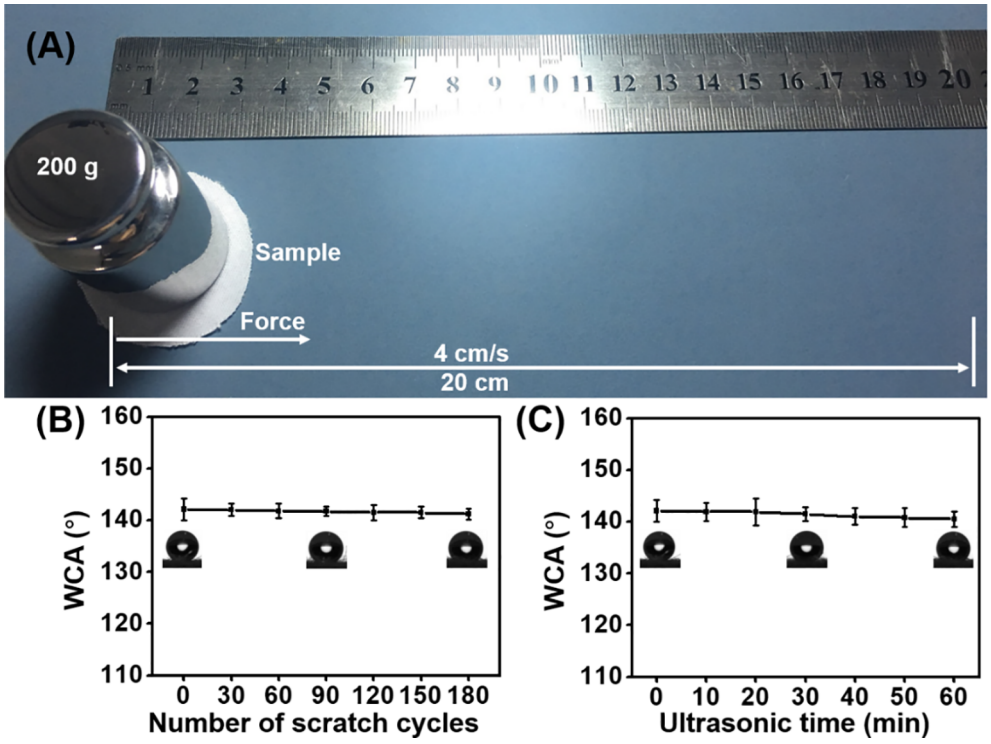

Fig. 5. (A) Schematic illustration of abrasion test for the modified fabric. Variation in the WCAs of the modified fabric after being (B) abraded by sandpaper and (C) washed under ultrasonic wave. Error bars represent the standard deviation of quintuplicate experiments.

environments seem unlikely to affect the elongation at break of fabrics (Table 1). Therefore, we conclude that the POSS modified fabric has excellent UV, chemical and mechanical stabilities at harsh environments.

3.5. Self-cleaning performance of the modified fabric

Compared to the original fabric, the modified fabric exhibits good self-cleaning performance. When the modified fabric was soaked into water, a mirror-like phenomenon (Fig. 6A) could be observed, which was owing to the trapped air onto the surface of modified fabric that established a solid–liquid–air interfaces [61]. After the modified fabric was taken out from the water, its surface was entirely dry. On the contrary, the original fabric was totally wetted by water because of its inherent hydrophilic feature and capillary effect [62]. We found that various water droplets (10 μL) in daily usage maintained spherical shape on the surface of modified fabric, while infiltrating into the original fabric (Fig. 6B and C). To verify the self-cleaning property of the modified fabric, Congo Red (CR) powders were employed as a marker on the surfaces [63]. It can be observed that there exists obvious difference between the original and modified fabric when CR powers are washed by water droplets. For the original fabric, dye powders stay on and pollute the surface. While for the modified fabric, dye powders can be taken away immediately when the water droplets slide over the surface (Fig. 6D and E). Meanwhile, after the dyed water droplets were dropped onto the modified surface, they could slip away immediately (Video S1), suggesting the weak interaction between them. Consequently, the excellent anti-staining ability of the modified fabric indicates that it can be used in the self-cleaning field [64].

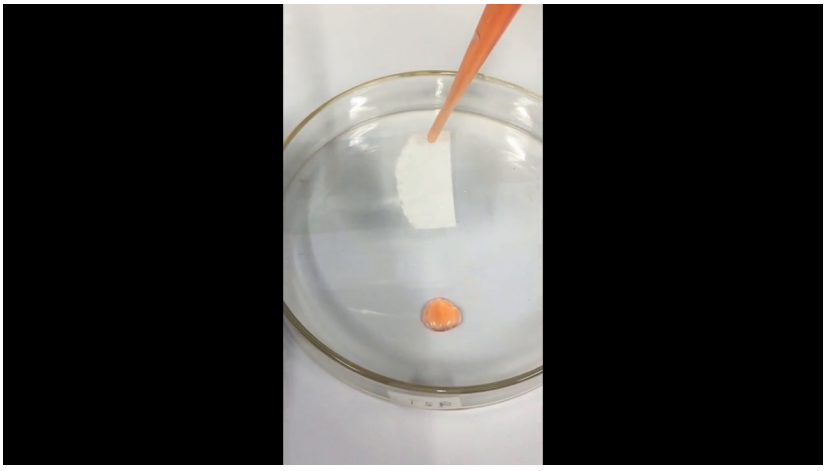

Video S1.

3.6. Oil/water separation property of the modified fabric

The surface tension of the modified fabric is around 56.3 mN/m, which is lower than that of water and higher that of oil [65]. Therefore, the modified fabric can be used for removing oil from water through absorption and separation. Fig. 7A illustrates the process of oil absorption. The Sudan III dyed chloroform can be absorbed immediately as it touches the modified fabric. To evaluate the absorption capacity, the weight gain of modified fabric for various oils was measured. As shown in Fig. 7C, the weight gain of modified fabric is around two times of its own weight. Besides, the modified fabric is a good candidate and can be used as selective filter membrane for separation of different oil/water mixtures, owing to its good hydrophilicity, oleophilicity and porous structure. As shown in Fig. 7B and Video S2, when chloroform (dyed by Sudan III)/water mixture was poured onto the surface of modified fabric, the chloroform phase sank into the lower layer due to its gravity force and then immediately permeated through without any external driven force, while the water was still retained above the fabric because of its hydrophobicity. To evaluate the water repellency, the water intrusion pressure (P) of modified fabric was calculated according to Eq. (4):

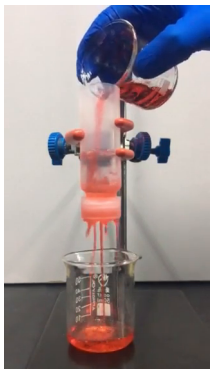

Video S2.

$$P = \rho g h_{max} \quad (4)$$

where ρ denotes the density of water, g is the acceleration of gravity, and h_{max} represents the maximum height of water that the modified fabric can support without penetration [66]. We found that the h_{max} of the modified fabric was 20.1 ± 0.3 cm (Video S3), corresponding to the calculated intrusion pressure of 1.97 ± 0.29 (KPa). It was found that the separation (η (%)) was higher than 99.1% even after 50 separation cycles (Fig. 7D). In the meantime, WCAs of the modified fabric were unchanged after the repeated separation process (Fig. 7D, inset). Additionally, the modified fabric can also be used for separation different oil/water mixtures, such as N-hexane/water mixture (light oil/water mixture), as shown in Video S4. The separation efficiencies of other different kinds of oil/water mixtures are displayed in Fig. 7E. We found that separation efficiency of different oil/water mixtures could maintain a high level. These results demonstrate the modified fabric is a good filtration material for oil/water separation.

Video S3.

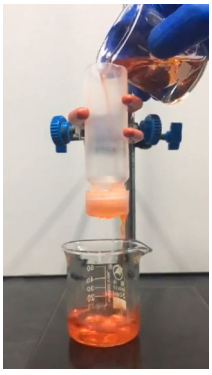

Video S4.

To satisfy the demands of pragmatic application, three typical oil/water mixtures of acid, alkali and salt including chloroform-1M H_2SO_4, chloroform-1M NaOH, and chloroform-saturated NaCl aqueous solution (1/1, v/v) were used to investigate the stability of oil/water separation of the modified fabric in harsh conditions. As displayed in Fig. 8A, B, C and Video S5–S7, the dyed chloroform can permeate through the fabric immediately with similar separation process as the normal chloroform/water mixture, while the aqueous solution was still retained. Additionally, Fig. 8D shows the separation efficiency of the modified fabric after different separation process. All of the oil/water mixtures could remain a high level (> 96%) even after 50 cycles of separation in harsh conditions. Based on these results, we conclude that the POSS modified fabric has great opportunity for oil/water separation, even in severe environments.

Video S5.

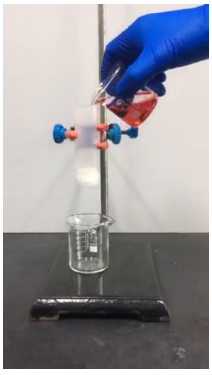

Video S6.

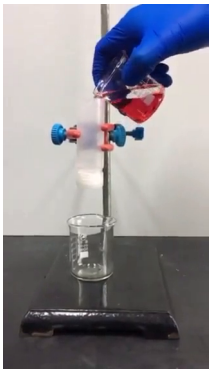

Video S7.

Apart from separation efficiency, permeate flux is another indispensable parameter to evaluate oil/water separation in industrial applications. Therefore, permeate fluxes of various oil/water mixtures were investigated. When the heavy oil/water mixtures were separated, the permeate fluxes of chloroform and dichloromethane could be reached to 114,744 and 111,121 $L{\cdot}m^{-2}{\cdot}h^{-1}$, respectively. As for the light oil/water mixtures, permeate fluxes of 93139, 92,859 and 74,161 $L{\cdot}m^{-2}{\cdot}h^{-1}$ can be achieved for petroleum ether, N-hexane and toluene, respectively. The fluxes in our research showed a remarkable superiority in comparison with other previous works, as shown in Table 2. The specific surface area and pore volume of the original and modified cotton fabrics were calculated using the mercury intrusion porosimeter (MIP, Pore Master 33, USA). Compared to the original fabric with the specific surface area and pore volume of 11.08 m^2/g and 1.52 cm^3/g, the values for the modified fabric are 5.08 m^2/g and 1.35 cm^3/g. The larger pore size and the oleophilic of modified maybe the reason of high

Table 1
Tensile strength and elongation at break of various fabrics.

Samples	Original fabric	Modified fabric	pH = 1 [a]	pH = 13[b]	DMF [c]	THF [d]	MeOH [e]	Acetone [f]	N-hexane [g]	UV [h]	Abrasion [i]
Tensile strength (N/cm^2)	4396 ± 8 (warp)	3472 ± 3 (warp)	3258 ± 5 (warp)	3085 ± 9 (warp)	3127 ± 5 (warp)	3317 ± 9 (warp)	3301 ± 7 (warp)	3182 ± 4 (warp)	3398 ± 5 (warp)	3465 ± 7 (warp)	3023 ± 6 (warp)
	1961 ± 10 (weft)	1550 ± 7 (weft)	1427 ± 8 (weft)	1402 ± 13 (weft)	1413 ± 8 (weft)	1451 ± 6 (weft)	1478 ± 9 (weft)	1411 ± 7 (weft)	1498 ± 5 (weft)	1539 ± 9 (weft)	1379 ± 13 (weft)
Elongation at break (%)	12.4 ± 0.9 (warp)	13.4 ± 1.1 (warp)	14.4 ± 0.8 (warp)	15.0 ± 1.4 (warp)	15.0 ± 0.7 (warp)	14.2 ± 1.5 (warp)	14.3 ± 1.2 (warp)	14.5 ± 1.4 (warp)	13.6 ± 0.7 (warp)	13.4 ± 1.0 (warp)	15.4 ± 1.6 (warp)
	32.4 ± 0.8 (weft)	33.4 ± 1.0 (weft)	35.9 ± 1.1 (weft)	36.4 ± 1.4 (weft)	36.5 ± 0.9 (weft)	35.2 ± 0.6 (weft)	34.7 ± 1.3 (weft)	36.1 ± 0.8 (weft)	34.6 ± 0.7 (weft)	33.6 ± 1.0 (weft)	37.5 ± 1.5 (weft)

[a] The modified fabric was immersed in pH = 1 solution for 72 h.
[b] The modified fabric was immersed in pH = 13 solution for 72 h.
[c] The modified fabric was treated in DMF solution for 72 h.
[d] The modified fabric was treated in THF solution for 72 h.
[e] The modified fabric was treated in MeOH solution for 72 h.
[f] The modified fabric was treated in Acetone solution for 72 h.
[g] The modified fabric was treated in N-hexane solution for 72 h.
[h] The modified fabric was radiated at UV light for 24 h.
[i] The modified fabric was rubbed for 180 cycles.

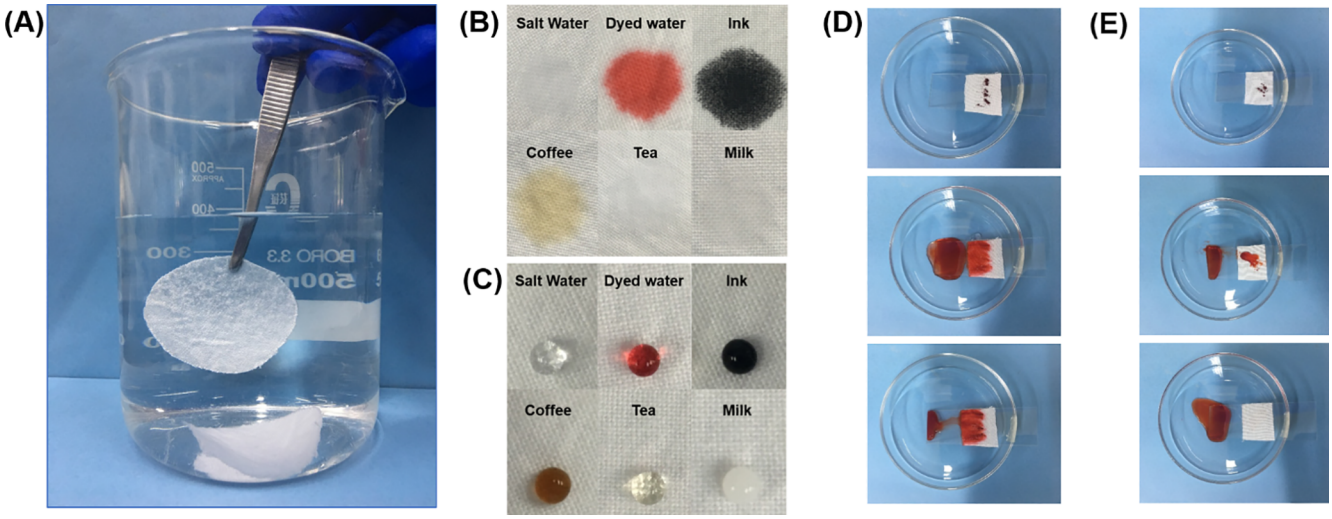

Fig. 6. (A) A mirror-like phenomenon was observed when the modified fabric was immersed in water, while the original fabric was totally wetted by water. Photographs of various domestic used solution droplets (10 μL) on the (B) original fabric and (C) modified fabric. Self-cleaning process of the (D) original fabric and (E) modified fabric.

flux compared to other substrates and nanoparticles [79]. Therefore, the modified fabric with extraordinary reusability and stability can be served as an ideal candidate for the demands of industrial separation due to its steadily outstanding separation efficiency and remarkable high-flux, even in harsh conditions.

4. Conclusions

In summary, a robust POSS based self-cleaning hydrophobic fabric has been successfully fabricated by a facile one-step dip-coating method. The anchored POSS onto the cotton fabric provide appropriate surface roughness and lowered surface energy, resulting in excellent hydrophobic performance of modified fabric. It was found that the modified fabric exhibited remarkable resistance against UV irradiation, chemical-corrosion, ultrasonically washed and mechanical abrasion. Solely driven by gravity, the modified fabric can enable separation of oil/water mixture with good separation efficiency and ultrahigh permeation flux. Besides, the modified fabric still maintained its high separation efficiencies in harsh conditions (such as acid, alkali, and salt solutions). These results tell us that the POSS modified fabric possesses strong stabilities against harsh environments and can deal with various oil-polluted solutions. Therefore, this facile strategy is of great importance in the preparation of robust hydrophobic filtration materials for oil/water separation.

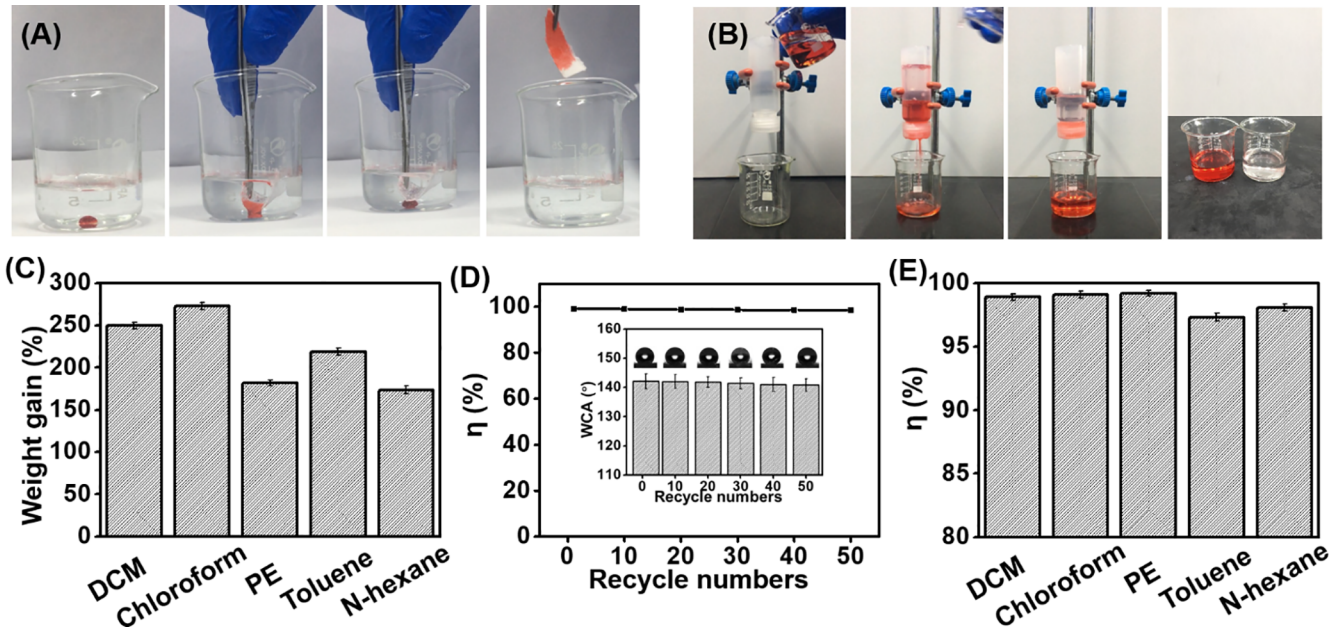

Fig. 7. (A) Selective absorption of the modified fabric for chloroform in water. (B) Separation process of the modified fabric for chloroform/water mixture. (C) Weight gain of the modified fabric for various types of oil. (D) Variation of the separation efficiency (for chloroform/water mixture) of the modified fabric after different recycle times, inset is WCA variation after different recycle times. (E) Separation efficiency for various oil/water mixtures, oils are dyed by Sudan III. Error bars represent the standard deviation of quintuplicate experiments.

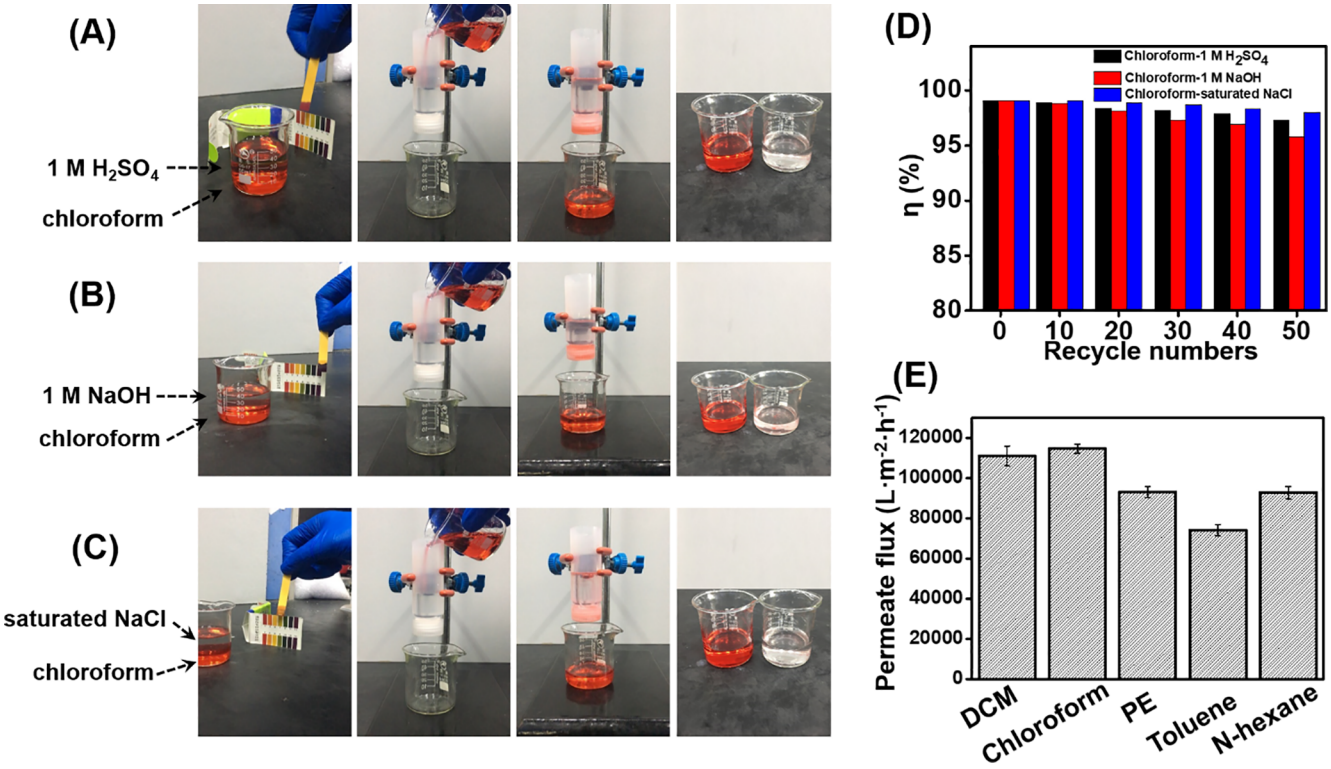

Fig. 8. Separation process of the modified fabric for (A) chloroform-1M H_2SO_4, (B) chloroform-1M NaOH, and (C) chloroform-saturated NaCl, chloroform is dyed by Sudan III. (D) Separation efficiency for three above oil/water mixtures after different recycle times. (E) Permeate flux of various mixtures for oil/water separation. Error bars represent the standard deviation of quintuplicate experiments.

Table 2
The permeation fluxes of various oil/water filtration materials.

Substrate	Material	Method	WCA (°)	Abrasion test (Y or N)	Driver	Flux ($L{\cdot}m^{-2}h^{-1}$)	Reference
Stainless steel mesh	Reduced graphene oxide (RGO)	Coated	153	Y	Gravity	1900	[67]
Stainless steel mesh	TiO_2	Sol-gel; dip-coating	150.8	N	Gravity	7281	[68]
Stainless steel mesh	Cu-Ni/pDOp/NDM	Electrodeposition	162	Y	Gravity	3000	[69]
Copper mesh	$Cu(OH)_2$ nanoneedles and CuO nanoplates	Surface oxidation	160.2	Y	Gravity	46,800	[70]
Copper mesh	Candle soot	Electrodeposition	153	Y	Gravity	4378	[71]
Copper mesh	Dopamine; 1-dodecanethiol	Dip-coating	152.4	N	Gravity	4507	[72]
Hydroxyapatite nanowire	HAP@Fe_3O_4@PDMS	Coated	154.8	Y	Gravity	2924.3	[73]
PVDF membrane	P(MMA-*r*-FDMA)	Electrospinning	155	N	Gravity	14,000	[74]
Polyester fabric	PVDF/PDA/PEI	non-solvent induced phase separation	153.3	N	0.02 MPa	7600	[75]
Cotton fabric	MPTES/MAPOSS	CVD; thiol-ene click chemistry	159	Y	–	–	[51]
Cotton fabric	ZnO/CESO/CFP/ STA	Dip-coated	156	N	Gravity	33,800	[76]
Cotton fabric	CESO/ CNC/HDTS	Dip-coating	157	N	Gravity	66,000	[77]
Cotton fabric	Fe_3O_4/LA-TiO_2	Dip-coating	153	N	Gravity	11,000	[78]
Cotton fabric	POSS	Dip-coating	142	Y	Gravity	114,744	This work

Acknowledgments

This work was financially supported by the National Natural Science Foundation of China (51721091). We thank the Analytical & Testing Center at Sichuan University in Chengdu, China, and Dr Gui-Ping Yuan, for assistance with TEM experiments.

Appendix A. Supplementary data

Supplementary data to this article can be found online at https://doi.org/10.1016/j.cej.2019.122391.

References

[1] S.B. Joye, Deepwater Horizon, 5 years on, Science 349 (2015) 592–593.
[2] I.B. Ivshina, M.S. Kuyukina, A.V. Krivoruchko, A.A. Elkin, S.O. Makarov, C.J. Cunningham, T.A. Peshkur, R.M. Atlas, J.C. Philp, Oil spill problems and sustainable response strategies through new technologies, Enviro. Sci.: Processes Impacts 17 (2015) 1201–1219.
[3] M.A. Shannon, P.W. Bohn, M. Elimelech, J.G. Georgiadis, B.J. Marinas, A.M. Mayes, Science and technology for water purification in the coming decades, Nature 452 (2008) 301–311.
[4] J. Aurell, B.K. Gullett, Aerostat sampling of PCDD/PCDF emissions from the Gulf oil spill in situ burns, Environ. Sci. Technol. 44 (2010) 9431–9437.
[5] R.K. Gupta, G.J. Dunderdale, M.W. England, A. Hozumi, Oil/water separation techniques: a review of recent progresses and future directions, J. Mater. Chem. A. 5 (2017) 16025–16058.
[6] A.K. Kota, G. Kwon, W. Choi, J.M. Mabry, A. Tuteja, Hygro-responsive membranes

for effective oil–water separation, Nat. Commun. 3 (2012) 1025.
[7] M. Kamali, D. Suhas, M.E. Costa, I. Capela, T.M. Aminabhavi, Sustainability considerations in membrane-based technologies for industrial effluents treatment, Chem. Eng. J. 368 (2019) 474–494.
[8] Y. Liu, G. Zeng, H. Zhong, Z. Wang, Z. Liu, M. Cheng, G. Liu, X. Yang, S. Liu, Effect of rhamnolipid solubilization on hexadecane bioavailability: enhancement or reduction? J. Hazard. Mater. 322 (2017) 394–401.
[9] Y. Liu, Z. Liu, D. Huang, M. Cheng, G. Zeng, C. Lai, C. Zhang, C. Zhou, W. Wang, D. Jiang, Metal or metal-containing nanoparticle@ MOF nanocomposites as a promising type of photocatalyst, Coord. Chem. Rev. 388 (2019) 63–78.
[10] B. Liang, G. Zhang, Z. Zhong, T. Sato, A. Hozumi, Z. Su, Substrate-independent polyzwitterionic coating for oil/water separation membranes, Chem. Eng. J. 362 (2019) 126–135.
[11] Z. Xue, Y. Cao, N. Liu, L. Feng, L. Jiang, Special wettable materials for oil/water separation, J. Mater. Chem. A 2 (2014) 2445–2460.
[12] X. Yue, Z. Li, T. Zhang, D. Yang, F. Qiu, Design and fabrication of superwetting fiber-based membranes for oil/water separation applications, Chem. Eng. J. 364 (2019) 292–309.
[13] Y. Jing, L. Zhang, R. Huang, D. Bai, H. Bai, Q. Zhang, Q. Fu, Ultrahigh-performance electrospun polylactide membranes with excellent oil/water separation ability via interfacial stereocomplex crystallization, J. Mater. Chem. A 5 (2017) 19729–19737.
[14] F.-F. Ma, N. Zhang, X. Wei, J.-H. Yang, Y. Wang, Z.-W. Zhou, Blend-electrospun poly (vinylidene fluoride)/polydopamine membranes: self-polymerization of dopamine and the excellent adsorption/separation abilities, J. Mater. Chem. A 5 (2017) 14430–14443.
[15] Y. Dou, D. Tian, Z. Sun, Q. Liu, N. Zhang, J.H. Kim, L. Jiang, S.X. Dou, Fish gill inspired crossflow for efficient and continuous collection of spilled oil, ACS Nano 11 (2017) 2477–2485.
[16] Z. Chu, Y. Feng, S. Seeger, Oil/water separation with selective superantiwetting/superwetting surface materials, Angew. Chem., Int. Ed. 54 (2015) 2328–2338.
[17] D.W. Kim, K. Eum, H. Kim, D. Kim, M.D. de Mello, K. Park, M. Tsapatsis, Continuous ZIF-8/reduced graphene oxide nanocoating for ultrafast oil/water separation, Chem. Eng. J. 372 (2019) 509–515.
[18] M. Liu, S. Wang, L. Jiang, Nature-inspired superwettability systems, Nat. Rev. Mater. 2 (2017) 17036.
[19] H. Guo, J. Yang, T. Xu, W. Zhao, J. Zhang, Y. Zhu, C. Wen, Q. Li, X. Sui, L. Zhang, A robust cotton textile based material for high flux oil-water separation, ACS Appl. Mater. Interfaces 11 (2019) 13704–13713.
[20] Y. Liu, Y. Su, J. Guan, J. Cao, R. Zhang, M. He, K. Gao, L. Zhou, Z. Jiang, 2D Heterostructure Membranes with Sunlight-Driven Self-Cleaning Ability for Highly Efficient Oil-Water Separation, Adv. Funct. Mater. 28 (2018) 1706545.
[21] F. Li, Z. Wang, S. Huang, Y. Pan, X. Zhao, Flexible, Durable, and Unconditioned Superoleophobic/Superhydrophilic Surfaces for Controllable Transport and Oil-Water Separation, Adv. Funct. Mater. 28 (2018) 1706867.
[22] W.S. Wong, Z.H. Stachurski, D.R. Nisbet, A. Tricoli, Ultra-durable and transparent self-cleaning surfaces by large-scale self-assembly of hierarchical interpenetrated polymer networks, ACS Appl. Mater. Interfaces 8 (2016) 13615–13623.
[23] S. Li, J. Huang, M. Ge, C. Cao, S. Deng, S. Zhang, G. Chen, K. Zhang, S.S. Al-Deyab, Y. Lai, Robust flower-like TiO_2@cotton fabrics with special wettability for effective self-cleaning and versatile oil/water separation, Adv. Mater. Interfaces 2 (2015) 1500220.
[24] J. Huang, S. Li, M. Ge, L. Wang, T. Xing, G. Chen, X. Liu, S.S. Al-Deyab, K. Zhang, T. Chen, Robust superhydrophobic TiO_2@fabrics for UV shielding, self-cleaning and oil–water separation, J. Mater. Chem. A 3 (2015) 2825–2832.
[25] D. Li, Z. Guo, Stable and self-healing superhydrophobic MnO_2@ fabrics: Applications in self-cleaning, oil/water separation and wear resistance, J. Colloid Interface Sci. 503 (2017) 124–130.
[26] M. Cheng, Y. Liu, D. Huang, C. Lai, G. Zeng, J. Huang, Z. Liu, C. Zhang, C. Zhou, L. Qin, Prussian blue analogue derived magnetic Cu-Fe oxide as a recyclable photo-Fenton catalyst for the efficient removal of sulfamethazine at near neutral pH values, Chem. Eng. J. 362 (2019) 865–876.
[27] X. Zhou, Z. Zhang, X. Xu, F. Guo, X. Zhu, X. Men, B. Ge, Robust and durable superhydrophobic cotton fabrics for oil/water separation, ACS Appl. Mater. Interfaces 5 (2013) 7208–7214.
[28] S.-W. Kuo, F.-C. Chang, POSS related polymer nanocomposites, Prog. Polym. Sci. 36 (2011) 1649–1696.
[29] R.M. Laine, M.F. Roll, Polyhedral phenylsilsesquioxanes, Macromolecules 44 (2011) 1073–1109.
[30] K. Tanaka, Y. Chujo, Advanced functional materials based on polyhedral oligomeric silsesquioxane (POSS), J. Mater. Chem. 22 (2012) 1733–1746.
[31] D. Han, T.-J. Wen, G. Han, Y.-Y. Deng, Y. Deng, Q. Zhang, Q. Fu, Synthesis of Janus POSS star polymer and exploring its compatibilization behavior for PLLA/PCL polymer blends, Polymer 136 (2018) 84–91.
[32] E. McMullin, H.T. Rebar, P.T. Mather, Biodegradable thermoplastic elastomers incorporating POSS: synthesis, microstructure, and mechanical properties, Macromolecules 49 (2016) 3769–3779.
[33] D. Han, Q. Zhang, F. Chen, Q. Fu, Using POSS–C_{60} giant molecules as a novel compatibilizer for PS/PMMA polymer blends, RSC Adv. 6 (2016) 18924–18928.
[34] X. Wang, L. Song, H. Yang, W. Xing, B. Kandola, Y. Hu, Simultaneous reduction and surface functionalization of graphene oxide with POSS for reducing fire hazards in epoxy composites, J. Mater. Chem. 22 (2012) 22037–22043.
[35] D. Han, Q.Y. Guo, W.-B. Zhang, L.-X. Liu, Q. Fu, Preparation and properties of polystyrene nanocomposites containing dumbbell-shaped molecular nanoparticles based on polyhedral oligomeric silsesquioxane and [60] fullerene, RSC Adv. 5 (2015) 70051–70058.
[36] W. Zhang, G. Camino, R. Yang, Polymer/polyhedral oligomeric silsesquioxane (POSS) nanocomposites: An overview of fire retardance, Prog. Polym. Sci. 67 (2017) 77–125.
[37] S. Zhang, X. Li, H. Fan, Q. Fu, Y. Gu, Epoxy nanocomposites: Improved thermal and dielectric properties by benzoxazinyl modified polyhedral oligomeric silsesquioxane, Mater. Chem. Phys. 223 (2019) 260–267.
[38] J. Yuan, Z. Zhang, M. Yang, W. Wang, X. Men, W. Liu, POSS grafted hybrid-fabric composites with a biomimic middle layer for simultaneously improved UV resistance and tribological properties, Compos. Sci. Technol. 160 (2018) 69–78.
[39] Y.-Y. Deng, D. Han, D.-L. Zhou, Z.-Q. Liu, Q. Zhang, Y. Li, Q. Fu, Monodispersed hybrid microparticles based on polyhedral oligomeric silsesquioxane with good UV resistance and high thermal stability: From organic to inorganic, Polymer 121609 (2019).
[40] Y. Xue, Y. Liu, F. Lu, J. Qu, H. Chen, L. Dai, Functionalization of graphene oxide with polyhedral oligomeric silsesquioxane (POSS) for multifunctional applications, J. Phys. Chem. Lett. 3 (2012) 1607–1612.
[41] Y. Xue, H. Wang, Y. Zhao, L. Dai, L. Feng, X. Wang, T. Lin, Magnetic liquid marbles: a “precise” miniature reactor, Adv. Mater. 22 (2010) 4814–4818.
[42] Y. Shao, H. Yin, X.-M. Wang, S.-Y. Han, X. Yan, J. Xu, J. He, P. Ni, W.-B. Zhang, Mixed [2: 6] hetero-arm star polymers based on Janus POSS with precisely defined arm distribution, Polym. Chem. 7 (2016) 2381–2388.
[43] D. Han, Y. Shao, Y.-D. Tao, G. Han, D.-L. Zhou, S. Yang, W.-B. Zhang, Q. Fu, Symmetry-guided, divergent assembly of regio-isomeric molecular Janus particles, Chem. Commun. (2019).
[44] G.-L. Zhu, D. Han, Y. Yuan, F. Chen, Q. Fu, Improving damping properties and thermal stability of epoxy/polyurethane grafted copolymer by adding glycidyl POSS, Chin. J. Polym. Sci. 36 (2018) 1297–1302.
[45] Y. Li, X.-H. Dong, Y. Zou, Z. Wang, K. Yue, M. Huang, H. Liu, X. Feng, Z. Lin, W. Zhang, W.-B. Zhang, S. Cheng, Polyhedral oligomeric silsesquioxane meets “click” chemistry: Rational design and facile preparation of functional hybrid materials, Polymer 125 (2017) 303–329.
[46] D.J. Krug, R.M. Laine, Durable and Hydrophobic Organic-Inorganic Hybrid Coatings via Fluoride Rearrangement of Phenyl T12 Silsesquioxane and Siloxanes, ACS Appl. Mater. Interfaces 9 (2017) 8378–8383.
[47] S. Foorginezhad, M.M. Zerafat, Fabrication of superhydrophobic coatings with self-cleaning properties on cotton fabric based on Octa vinyl polyhedral oligomeric silsesquioxane/polydimethylsiloxane (OV-POSS/PDMS) nanocomposite, J. Colloid Interface Sci. 540 (2019) 78–87.
[48] P. Pi, K. Hou, X. Wen, S. Xu, J. Cheng, G. Xu, S. Wang, A facile one-step fabrication of robust superhydrophobic/superoleophilic cotton fabric using a crosslinkable POSS-containing fluorinated copolymer, Prog. Org. Coat. 101 (2016) 522–529.
[49] C. Zhang, P. Li, B. Cao, Electrospun microfibrous membranes based on PIM-1/POSS with high oil wettability for separation of oil–water mixtures and cleanup of oil soluble contaminants, Ind. Eng. Chem. Res. 54 (2015) 8772–8781.
[50] H. Wang, Y. Xue, J. Ding, L. Feng, X. Wang, T. Lin, Durable self-healing superhydrophobic and superoleophobic surfaces from fluorinated-decyl polyhedral oligomeric silsesquioxane and hydrolyzed fluorinated alkyl silane, Angew. Chem., Int. Ed. 50 (2011) 11433–11436.
[51] K. Hou, Y. Zeng, C. Zhou, J. Chen, X. Wen, S. Xu, J. Cheng, P. Pi, Facile generation of robust POSS-based superhydrophobic fabrics via thiol-ene click chemistry, Chem. Eng. J. 332 (2018) 150–159.
[52] H. Shi, D. Shi, L. Yin, Z. Yang, S. Luan, J. Gao, J. Zha, J. Yin, R.K. Li, Ultrasonication assisted preparation of carbonaceous nanoparticles modified polyurethane foam with good conductivity and high oil absorption properties, Nanoscale 6 (2014) 13748–13753.
[53] Y. Cao, X. Zhang, L. Tao, K. Li, Z. Xue, L. Feng, Y. Wei, Mussel-inspired chemistry and michael addition reaction for efficient oil/water separation, ACS Appl. Mater. Interfaces 5 (2013) 4438–4442.
[54] C. Zhou, Z. Chen, H. Yang, K. Hou, X. Zeng, Y. Zheng, J. Cheng, Nature-inspired strategy toward superhydrophobic fabrics for versatile oil/water separation, ACS Appl. Mater. Interfaces 9 (2017) 9184–9194.
[55] L. Aljerf, High-efficiency extraction of bromocresol purple dye and heavy metals as chromium from industrial effluent by adsorption onto a modified surface of zeolite: kinetics and equilibrium study, J. Environ. Manag. 225 (2018) 120–132.
[56] F. Guo, L. Schulte, M.E. Vigild, S. Ndoni, Load–release of small and macromolecules from elastomers with reversible gyroid mesoporosity, Soft Matter 8 (2012) 11499–11507.
[57] S. Yang, L. Zhang, Q. Yang, Z. Zhang, B. Chen, P. Lv, W. Zhu, G. Wang, Graphene aerogel prepared by thermal evaporation of graphene oxide suspension containing sodium bicarbonate, J. Mater. Chem. A 3 (2015) 7950–7958.
[58] J. Yong, F. Chen, Q. Yang, J. Huo, X. Hou, Superoleophobic surfaces, Chem. Soc. Rev. 46 (2017) 4168–4217.
[59] G.B. Darband, M. Aliofkhazraei, S. Khorsand, S. Sokhanvar, A. Kaboli, Science and engineering of superhydrophobic surfaces: review of corrosion resistance, chemical and mechanical stability, Arab. J. Chem. (2018), https://doi.org/10.1016/j.arabjc.2018.01.013.
[60] C. Cao, M. Ge, J. Huang, S. Li, S. Deng, S. Zhang, Z. Chen, K. Zhang, S.S. Al-Deyab, Y. Lai, Robust fluorine-free superhydrophobic PDMS–ormosil@fabrics for highly effective self-cleaning and efficient oil–water separation, J. Mater. Chem. A 4 (2016) 12179–12187.
[61] W. Qiu, D. Xu, B. Liu, L. Shen, Q. Guo, Fabrication of superhydrophobic surfaces by smoke deposition and application in oil–water separation, RSC Adv. 5 (2015) 71329–71335.
[62] S. Bouaidat, O. Hansen, H. Bruus, C. Berendsen, N.K. Bau-Madsen, P. Thomsen, A. Wolff, J. Jonsmann, Surface-directed capillary system; theory, experiments and applications, Lab Chip 5 (2005) 827–836.
[63] A. Tombesi, S. Li, S. Sathasivam, K. Page, F.L. Heale, C. Pettinari, C.J. Carmalt, I.P. Parkin, Aerosol-assisted chemical vapour deposition of transparent superhydrophobic film by using mixed functional alkoxysilanes, Sci. Rep. 9 (2019) 7549.
[64] S.R. Saad, N. Mahmed, M.M.A.B. Abdullah, A.V. Sandu, Self-cleaning technology in fabric: A review, IOP Conf. Ser.: Mater. Sci. Eng. 133 (2016) 012028.
[65] J. Ma, A.P. Kalenak, A.G. Wong-Foy, A.J. Matzger, Rapid guest exchange and ultra-low surface tension solvents optimize metal-organic framework activation, Angew. Chem., Int. Ed. 56 (2017) 14618–14621.
[66] J. Huang, D. Yu, X. Xu, M. Liu, Z. Ye, G. Yang, T. Chen, H. Yang, J. Wang, X. Wu,

Ultra-high flux and efficient oil-water separation via polymer-based electrophoretic deposition, Chem. Eng. J. 371 (2019) 575–582.
[67] J. Chen, K. Li, H. Zhang, J. Liu, S. Wu, Q. Fan, H. Xue, Highly efficient and robust oil/water separation materials based on wire mesh coated by reduced graphene oxide, Langmuir 33 (2017) 9590–9597.
[68] X. Du, S. You, X. Wang, Q. Wang, J. Lu, Switchable and simultaneous oil/water separation induced by prewetting with a superamphiphilic self-cleaning mesh, Chem. Eng. J. 313 (2017) 398–403.
[69] M. Xiang, M. Jiang, Y. Zhang, Y. Liu, F. Shen, G. Yang, Y. He, L. Wang, X. Zhang, S. Deng, Fabrication of a novel superhydrophobic and superoleophilic surface by one-step electrodeposition method for continuous oil/water separation, Appl. Surf. Sci. 434 (2018) 1015–1020.
[70] B. Pang, H. Liu, P. Liu, H. Zhang, G. Avramidis, L. Chen, X. Deng, W. Viöl, K. Zhang, Robust, easy-cleaning superhydrophobic/superoleophilic copper meshes for oil/water separation under harsh conditions, Adv. Mater. Interfaces (2019) 1900158.
[71] H. Cao, J. Fu, Y. Liu, S. Chen, Facile design of superhydrophobic and superoleophilic copper mesh assisted by candle soot for oil water separation, Colloids Surf. A 537 (2018) 294–302.
[72] H. Cao, W. Gu, J. Fu, Y. Liu, S. Chen, Preparation of superhydrophobic/oleophilic copper mesh for oil-water separation, Appl. Surf. Sci. 412 (2017) 599–605.
[73] R.-L. Yang, Y.-J. Zhu, F.-F. Chen, D.-D. Qin, Z.-C. Xiong, Recyclable, fire-resistant, superhydrophobic, and magnetic paper based on ultralong hydroxyapatite nanowires for continuous oil/water separation and oil collection, ACS Sustainable Chem. Eng. 6 (2018) 10140–10150.
[74] I. Sadeghi, N. Govinna, P. Cebe, A. Asatekin, Superoleophilic, mechanically strong electrospun membranes for fast and efficient gravity-driven oil/water separation, ACS Appl. Polym. Mater. 1 (2019) 765–776.
[75] H.-M. Song, C. Chen, X.-X. Shui, H. Yang, L.-J. Zhu, Z.-X. Zeng, Q.-J. Xue, Asymmetric Janus membranes based on in situ mussel-inspired chemistry for efficient oil/water separation, J. Membrane Sci. 573 (2019) 126–134.
[76] Q.-Y. Cheng, X.-P. An, Y.-D. Li, C.-L. Huang, J.-B. Zeng, Sustainable and biodegradable superhydrophobic coating from epoxidized soybean oil and ZnO nanoparticles on cellulosic substrates for efficient oil/water separation, ACS Sustainable Chem. Eng. 5 (2017) 11440–11450.
[77] Q.-Y. Cheng, C.-S. Guan, M. Wang, Y.-D. Li, J.-B. Zeng, Cellulose nanocrystal coated cotton fabric with superhydrophobicity for efficient oil/water separation, Carbohydr. Polym. 199 (2018) 390–396.
[78] T. Yan, X. Chen, T. Zhang, J. Yu, X. Jiang, W. Hu, F. Jiao, A magnetic pH-induced textile fabric with switchable wettability for intelligent oil/water separation, Chem. Eng. J. 347 (2018) 52–63.
[79] Y. Ye, M. Tian, C. Zhang, Z. Du, J. Mi, Understanding controls on wetting at fluorinated polyhedral oligomeric silsesquioxane/polymer surfaces, Langmuir 32 (2015) 230–238.